

Thin film heat flux sensors for accurate transient and unidirectional heat transfer analysis

B Azerou, B Garnier, J Lahmar

Laboratoire de Thermocinétique, UMR CNRS 6607, Ecole Polytechnique de l'Université de Nantes, rue Christian Pauc, 44300 Nantes, France

E-mail: boussad.azerou@univ-nantes.fr; bertrand.garnier@univ-nantes.fr; abdeljalil.lahmar@univ-nantes.fr

Abstract. Heat flux measurement is needed in many heat transfer studies. For the best unbiased heat flux sensors (HFS), the heat flux is obtained using temperature measurements at different locations and also an inverse heat conduction method (function specification...) in order to calculate the heat flux. Systematic errors can come from the uncertainty in the wire thermocouples locations and from errors in the knowledge of distances between two consecutive wire thermocouples. The main idea in this work is to use thin film thermoresistances deposited on a flexible thin polymer substrate instead of wire thermocouples welded on metallic sample. The interest of using thin film thermoresistances instead of wire thermocouples is a lower disturbance due to the smaller thickness of the thin film sensors (typically less than $1\mu\text{m}$) and a much better knowledge of the distances between the different thin film thermoresistances which are precisely defined in the mask used for the metallic thin film pattern fabrication. In this paper, we present the fabrication of the new heat flux sensor with thin film thermoresistances, the study of the effect of the self heating (due to Joule effect in thermoresistances) and the performances of this new HFS with the comparison with classical HFS using wire thermocouples. For this study, a symmetric experimental setup is used with metallic samples equipped with an etched foil heater and both classical and new HFS. For several heating conditions, it appears that a better accuracy is always obtained with the new HFS using thin film thermoresistances.

1. Introduction

Heat flux sensors are very useful to understand and control the thermal phenomena coupled or not with other physical, chemical or mechanical processes. Heat flux sensor should be judiciously designed to insure the highest sensitivity and also to reduce sources of bias in the thermal quantities investigated (temperature, heat flux...).

Heat flux can be measured using direct methods, thus there exist heat flux sensors with normal or tangential gradient, and with electric dissipation or enthalpic technique [1, 3]. The gradient method frequently used is based on Fourier's conduction law, in which the heat flux is proportional to the thermal conductivity and to the temperature gradient. In most of the commercially available HFS, the temperature gradient is measured using thin film thermocouples deposited on both sides of a thin polymer layer (usually polyimide). However, those sensors are very often located directly on the medium to be characterized and the sensor creates more or less disturbance of the convective - radiative heat transfer between the medium and its surroundings. For example using such HFS sensor, Khaled et al. [4] have found a thermal disturbance which creates a 8% bias on the heat flux

measurement. For a more difficult case of one-dimensional transient heat flux measurement in metallic materials, there exists one type of heat flux sensor which was designed especially to reduce thermal disturbance generated by HFS sensor [5]. This heat flux sensor is composed of two half-shells made with the same material as the medium to characterize. A set of micro-thermocouples is installed in the cutting plane at different distances from the surface. The transient temperature distributions are used to estimate heat flux, using appropriate inverse methods such as function specification, Tikhonov regularization, mollification... [6-10]. As the cutting plane is parallel to the direction of the heat flow, the thermal disturbance is small especially for 1D heat transfer with a direction perpendicular to the surface. Previous studies about this type of sensor are about its design (size of the sensors, location of thermocouples) or its use in various situations [5, 11].

In recent years, the various energy saving programs present new measurement challenges in the field of heat transfer. A better management of heat transfer requires the development of more accurate heat flux sensors. Different new techniques of heat flux measurements have been developed and applied, which have greatly increased the resolution and operating range of heat flux instrumentation. Examples of recent advances in these areas were discussed in detail in numerous articles which review the design, the fabrication of HF sensors and the available heat flux measurement devices [12, 13]. There are different thin film HFS: thin film electrical resistance sensors [13-16], thin film gages sensors [17-19], thin film thermocouple sensors [19-23], and differential thermopile sensors [24-27].

The objective of this work is to design, realize and test a new type of heat flux sensor using thin film thermoresistances. With this new HFS, it is expected to obtain less biased in the heat flux measurement. Indeed, in heat flux sensor with wire thermocouples, considering the diameter of the thermocouples around 50 μm , there is some lack of accuracy in the localization of the thermocouple wires welded on the metallic wall, this results in an uncertainty about 25 μm for the distance between two consecutive thermocouple wires, it is hard to see where is exactly the welding. With thin film technology, the uncertainty for the distance between two consecutive thermoresistances is less than 5 μm , it is set during the masks manufacturing for the realization of the electrical pattern of the HFS. So, better accuracy is expected. One should notice that another advantage of using this thin film HFS is the facility to realize at the same time several HFS reducing cost fabrication compared to the classical thermocouple wires HFS. In this work, we present first the design and fabrication of the new heat flux sensor using thin film thermoresistances, then, the study of the effect of the self heating (due to Joule effect in thermoresistances) and finally the study of the performances of this new HFS with the comparison with classical HFS using thermocouple wires.

2. Fabrication and calibration of the new heat flux sensor.

2.1. Design and manufacture of thin film heat flux sensor

We have chosen to deposit thermoresistances instead of thin film thermocouples because thermoresistances require the deposition of only one material (copper here) and their sensitivity can be adjusted by varying the intensity of the current flowing through them.

Temperature measurements for the new heat flux sensor are performed with 9 μm thick copper thin film thermoresistances deposited on a polyimide substrate, 25 μm thick. The soft photolithography process was used to obtain a specific pattern (Figures 1 and 2) for the copper thermoresistances with a resolution about 3 μm . A very thin cold tinning (about 0.3 μm) is then performed on copper to prevent any copper oxydation and to increase the weldability.

Figure 3 shows the electrical pattern of one thermoresistance. The central thermoresistive element has a length of 20 μm and a width of 30 μm .

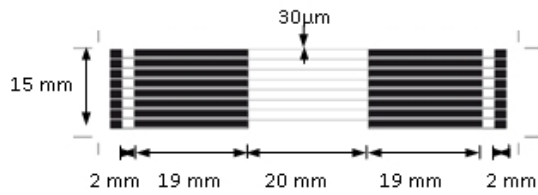


Figure 1. Mask for the thermoresistance network of the new thin film heat flux sensor.

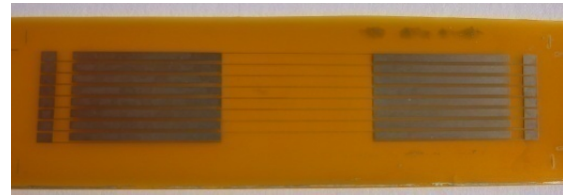


Figure 2. Polyimide substrate instrumented with 8 thin film thermoresistances (new HFS)

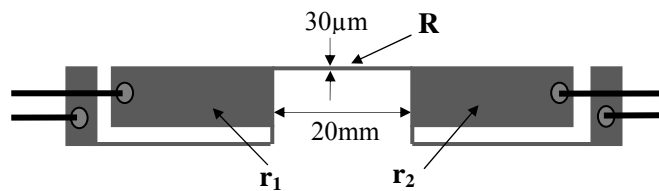


Figure 3. Electrical pattern of one thermoresistance

2.2. Thermoresistance calibration

Thin film thermoresistances of the new HFS are connected to Wheatstone bridges realized with electrical resistances fixed on an aluminum plate maintained at constant temperature (16 °C) using a refrigerated/heated water circulator. For the calibration of thermoresistances, relationships between the Wheatstone bridge unbalanced voltages ΔE divided by its voltage supply ΔV and the temperature T of the thermoresistances are sought for. A battery with electrical resistances (to lower the voltage) provides the voltage supply of the Wheatstone bridges, the voltage ΔU was kept constant during the calibration ($\Delta U \approx 46.0$ mV).

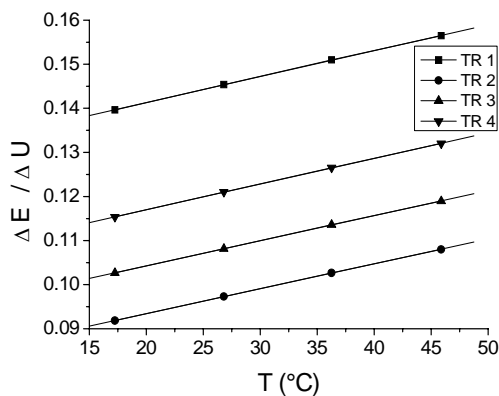


Figure 4. Calibration of 4 thin film thermoresistances (TR) of the new HFS

Table 1. Calibration for four thermoresistances of a heat flux sensor, $\Delta E/\Delta U = aT+b$

TR #	$a \cdot 10^4 (K^{-1})$	b	$\alpha \cdot 10^3 (K^{-1})$
TR1	5.883	0.12957	1.862
TR2	5.641	0.08215	1.785
TR3	5.701	0.09286	1.804
TR4	5.815	0.10537	1.841

Table 2. Locations of thermocouples (TH) and thermoresistances (TR) for the three HFS with respect to the surface of the stainless steel part

TR Location (mm)	TR1	TR2	TR3	TR4
	0.065	1.765	3.465	5.165
TH Location (mm)	TH1	TH2	TH3	TH4
	0.5945	2.577	6.607	12.607
TH Location (mm)	TH5	TH6	TH7	TH8
	0.44	2.507	6.45	12.44

For the calibration, the HFS was introduced between two instrumented aluminum blocks. The temperature of the aluminum blocks on each sides of the HFS, the unbalanced voltages ΔE of the Wheatstone bridges, therefore of each thermoresistances, and the voltage supply ΔV were measured using National Instruments data acquisition system (High - Speed M Series Multifunction DAQ for

USB – 16 - Bit) and amplifiers ANS with a gain, $G = 1000$ and a cutting frequency f_c of 10 Hz. A LabVIEW application software was used for data acquisition and recording.

Figure 4 shows the calibration of four thermoresistances of one HFS. One can notice linear relationships between the voltage ratio $\Delta E/\Delta U$ and the temperature of four thermoresistances of one HFS: $\Delta E/\Delta U = aT + b$. Finally the sensitivity of the thermal sensors is the product $a \cdot \Delta U$ which is here about $26.15 \mu\text{V}\cdot\text{K}^{-1}$ for a 19 mA current intensity through each thermoresistance. This sensitivity is lower than the one of bulk type K thermocouple. In addition, knowing the values of the electrical resistances in the Wheatstone bridge, one can deduce the temperature coefficient α of the copper thin film. As shown in Table 1, the average temperature coefficient α of the electrical resistivity of tinned copper thin film is about $1.82 \cdot 10^{-3} \text{K}^{-1}$ which is lower than the one of bulk copper ($3.93 \cdot 10^{-3} \text{K}^{-1}$).

3. Calculation of the Joule effect and parasitic self-heating

One drawback of using thermoresistances is that they need conditioning circuits to detect the variation of the copper thin film electrical resistance with temperature. So, it implies an electrical current circulation through thermal sensors and therefore an unwanted self heating of the thermoresistance due to Joule effect. This can create systematic errors in temperature measurement. Therefore it is important to quantify temperature biases as well as the power generated [14], especially for the central elements (R - figure 5), which have the greatest resistances.

The temperature rise induced in the central element was obtained by numerical simulations considering only one thermoresistance. Thus, the coupling between the electrical and thermal equations within the medium and copper thin layer was modeled with finite elements software (COMSOL Multiphysics 3.4), using the thin film approximation for the copper layer. Figure 5 shows the geometry and boundary conditions used in the electro-thermal model developed for one thermoresistive sensor. A parametric study was conducted by varying the electrical current through the thermoresistance between 1 and 100 mA by changing the supply voltage U.

Figure 6 shows Joule effect and the average and maximal temperature rises in the central element of the thermoresistance. One can observe that temperature rises are lower than 0.1°C if the current is smaller than 24 mA. For the previous calibration (Figure 4) and also for the following work, a current intensity about 19 mA was finally chosen through each thermoresistance resulting in a temperature bias lower than 0.06°C .

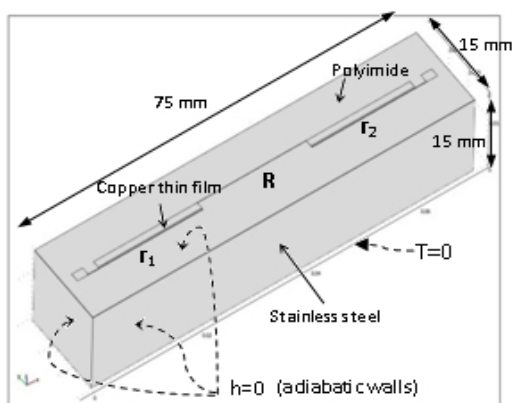


Figure 5. Physical electro-thermal model

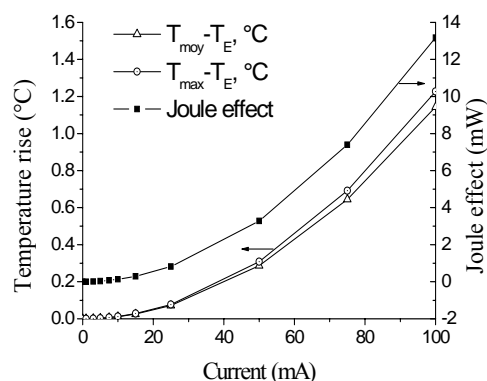


Figure 6. Temperature rise and Joule effect.

4. Experimental setup for the analysis of HFS performances

A symmetrical setup was designed to compare thin film thermoresistance HFS with an electric heater and then with classical wire thermocouple HFS (figure 7). This setup has an etched copper foil heater ($R = 11.22 \Omega$) surrounded by thin aluminum plates (2 mm thick) and then stainless steel parts between

which classical and new HFS were introduced. On the cold sides of the stainless steel parts are located aluminum plates and then heat exchangers with refrigerated or heated water circulator at 16°C. The various components of the device were separated by silicone grease to facilitate heat transfer. The two classical HFS were composed of a network of four - type K and 80 μm diam. - wire thermocouples welded on stainless steel parts 15mm thick. Between two other stainless steel parts is located a new HFS with thin film thermoresistances. The locations of thermocouples and thermoresistances for the three HFS are presented in Table 2 with respect to the surface of the stainless steel part close to the etched foil heater.

As shown in Figure 7, the two types of sensors were installed on the upper part of the experimental setup. By applying the voltage in the etched copper foil heater, heat dissipates more or less symmetrically on both sides, this will be quantified in the following.

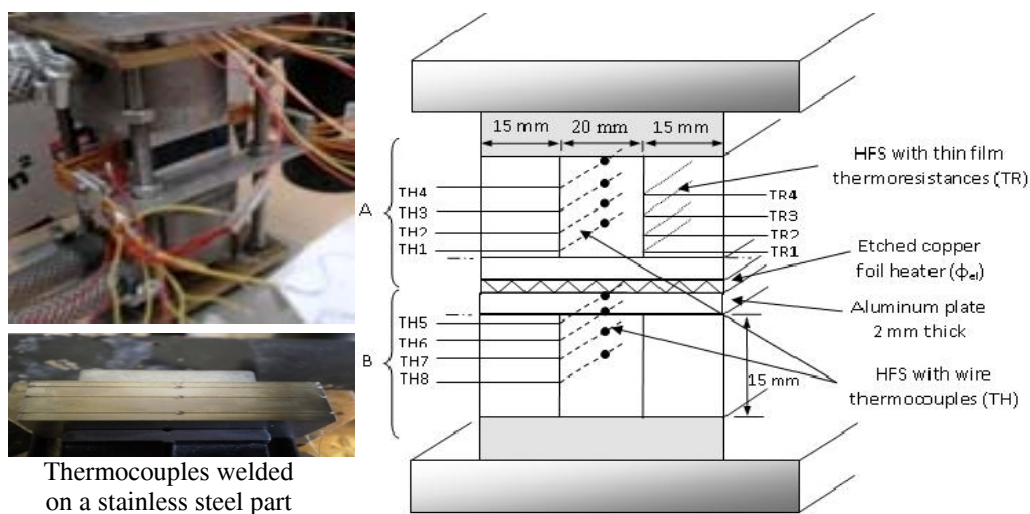


Figure 7. Experimental setup

5. Preliminary tests: symmetry of the device

The tests were conducted as follows: first we have fixed the supply voltage of the heater and then after waiting for steady state, we have measured the various temperatures (TH1 to TH8) delivered by the type K thermocouples (sensitivity of 40.87 $\mu\text{V}\cdot\text{K}^{-1}$). The heat flux in the etched copper foil heater is computed using the current intensity and supply voltage measurements. The heat flux through the classical HFS, i.e. with wire thermocouples, are computed using Fourier's law knowing the 2 following quantities:

- the thermal conductivity of stainless steel ($k = 14.8 \text{ W}\cdot\text{m}^{-1}\cdot\text{K}^{-1}$) measured using laser flash method [28] and,
- the temperature gradients within the two classical HFS using linear regressions with temperature measurements from thermocouples TH1 to TH8.

Table 3. Results for the analysis of the symmetry of the experimental setup.

U_{heat} (Volt)	φ_A (W/m^2)	φ_B (W/m^2)	$(\varphi_A + \varphi_B)$ (W/m^2)	φ_{el} (W/m^2)	$ ((\varphi_A + \varphi_B) - \varphi_{\text{el}})/\varphi_{\text{el}} $ (%)	$\varphi_A / (\varphi_A + \varphi_B)$ (%)	$\varphi_B / (\varphi_A + \varphi_B)$ (%)
10	1674.4	1694.6	3369	3440	2	49.7	50.3
20	6577.7	6773.6	13351.3	13726.4	2.7	49.27	50.73
30	14469.1	15047.7	29516.8	30502.6	3.2	49.02	50.98

Table 3 shows the different results according to the supply voltage U_{heat} of the etched copper foil heater. One can see that the total heat flux measured is close to the heat flux generated (2 to 3.2 %

discrepancy). However, the heat flux flowing through the lower part of the device is slightly higher than the one flowing in the upper part (discrepancy lower than 1%). This shows the quality of realization of this experimental setup with heat flux sensors.

6. Transient heat flux measurement

The evolutions of the heat fluxes, φ_{TR} and φ_{TH} , for transient measurement were obtained using temperature measurements in the stainless steel parts and an inverse heat conduction method. We have used the function specification method [6-9] which is sequential in nature and thus is computationally efficient. An algorithm solving the 1D heat conduction equation and using function specification method has been implemented with the Matlab software, considering a stainless steel part with constant thermal properties ($k= 14.81 \text{ W.m}^{-1}.\text{K}^{-1}$, $\rho = 7900 \text{ kg.m}^{-3}$ and $e = 15 \text{ mm}$) submitted to a heating of 100 s duration. In the 1D heat conduction model, the boundary conditions are unknown heat flux $\varphi(t)$ at $x = 0$ and measured temperature #4 (TR4 or TH4) at $x = x_4$ as illustrated on figure 8. The other parameters involved in the function specification method are: the computed time step (0.1 s), the spatial step (0.1 mm), the number of future time step (5) and the number of temperature sensors (4 for HFS with thermoresistances or wire thermocouples).

Figure 9 and figure 10 present the measured temperature and the heat flux obtained for the two types of heat flux sensors, i.e. with thermoresistances and with wire thermocouples. These measurements were obtained for a 100s heating with a voltage U_{heat} of 20V and a 50Hz sampling rate. The temperature and heat flux evolutions seem to be very similar.

Tables 4 and 5 present values concerning respectively the heat flux and the temperatures obtained with the two types of heat flux sensor and for steady state. Thus, it appears that the difference between heat flux dissipated electrically and measured heat flux is lower with the HFS with thin film thermoresistances (discrepancy between 1.5 and 1.8 %) than with the HFS with thermocouples (differences between 2.7 and 4.1 %). Otherwise, one can see that the standard deviations of the temperature and heat flux measurements are substantially identical for the two types of heat flux sensors, thus showing similar background noises.

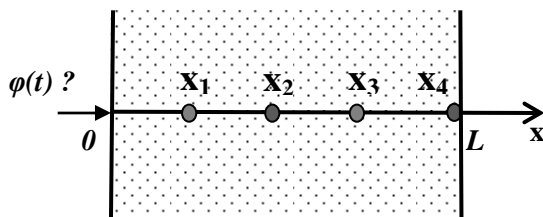


Figure 8. Heat flux estimation and boundary conditions

Table 4. Experimental time constants with the two types of temperature measurement

Sensor reference	TR τ (s)	TH τ (s)
TR1 or TH1	175.25	174.39
TR2 or TH2	174.9	173.3
TR3 or TH3	176.84	173.54
TR4 or TH4	175.96	174.37

7. Time constants

It is interesting to compare both types of sensor using non stationary temperature evolutions. The time constant of our system (heater, aluminium plates, stainless steel samples, heat exchangers...) was found using temperature measurements (TR and TH) performed with a heating voltage of 30 Volts during 800s. In Table 4, we can see that the time constants don't depend much on the thermocouple or thermoresistance reference that means on their locations. In addition, it appears that time constants with thermoresistance measurements are a little bit higher (0.3 to 1 %) than these with thermocouple measurements which is not very significant. The fact that it is a little bit higher can come from the polymer layers (black paint 8 μm and polyimide 25 μm thick) and the contact resistances which separate thermoresistances from the stainless steel parts. These polymers layers and contact resistance does not affect the heat flux flowing through the stainless steel parts in the main direction (vertical in figure 7) since polymers layers and contact surfaces are parallel to the main heat flow direction but the system time constant measured experimentally with thermoresistance is slightly affected.

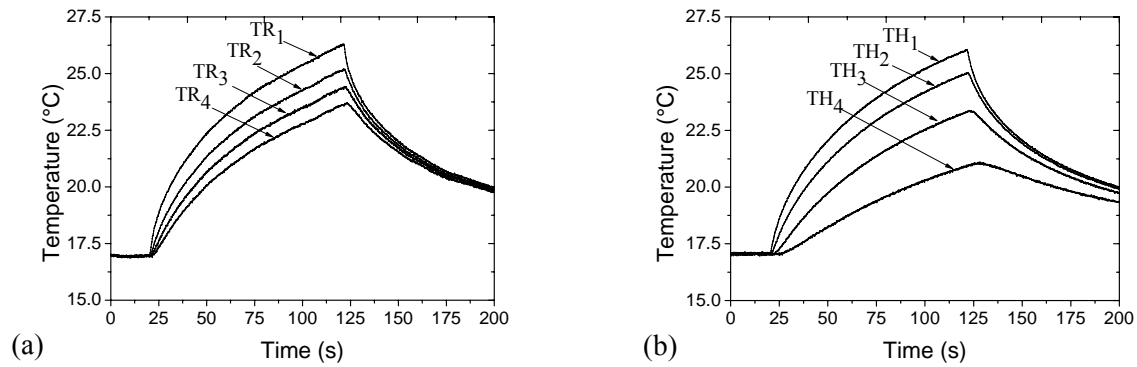


Figure 9. Measured temperature distributions using (a) thermoresistances -TR- or (b) wire thermocouples -TH-.

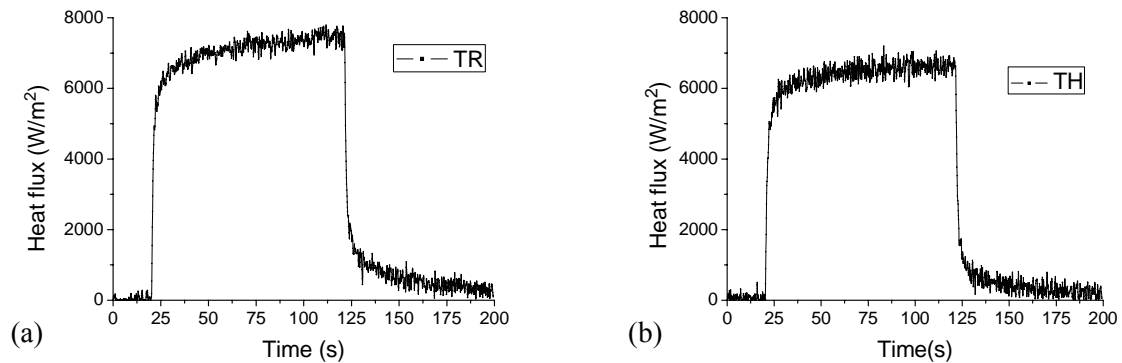


Figure 10. Estimated heat Flux with HFS using (a) thermoresistances-TR- or (b) wire thermocouples -TH-, following the application of a double level flux (duration 100 s, $U_{heat} = 20$ Volt)

Table 5. Heat flux estimated for the two types of HFS (σ : standard deviation, ϕ : heat flux, TR: thermoresistance, TH: thermocouple. The analyzed values are averaged ones over a period of 4 s before the end of the 100 s heating time).

		HFS with thermoresistances (TR)			HFS with wire thermocouples (TH)		
U_{heat} (Volt)	$\phi_{el}/2$ (W/m^2)	ϕ_{TR} estimated* (W/m^2)	σ_{TR} (W/m^2)	Error/ $(\phi_{el}/2)$ (%)	ϕ_{TH} estimated* (W/m^2)	σ_{TH} (W/m^2)	Error/ $(\phi_{el}/2)$ (%)
10	1681.5	1653.3	0.154	1.7	1726.1	0.177	2.7
20	6829.8	7113.7	0.186	1.8	6950.4	0.199	4.1
30	15206.0	15341.4	0.014	1.5	15659.3	0.019	3

*: average 4s

Table 6. Temperatures measured by the sensor close to the surface for the two HFS and for steady state (the analyzed values are average ones over a period of 4 s before the end of the 100s heating time).

		HFS with thermoresistances (TR)		HFS with wire thermocouples (TH)	
U_{heat} (Volt)		TR1* ($^{\circ}C$)	σ_{TR1} ($^{\circ}C$)	TH1* ($^{\circ}C$)	σ_{TH1} ($^{\circ}C$)
10		2.23	0.027	2.22	0.019
20		9.45	0.048	8.85	0.048
30		20.78	0.095	20.10	0.100

*: average over 4s

8. Conclusions

A new thin film heat flux sensor has been designed, fabricated, calibrated and tested. It is based on the use of thin film copper thermoresistances. The new heat flux sensor turns out to be more accurate than the conventional heat flux sensor with wire thermocouples, this come probably from the better knowledge of the location of various thermoresistances. The overheating of the thermoresistances due to Joule heating has been calculated and the current adjusted to control temperature measurement error. No significant change in response time could be found. In addition, thanks to the manufacturing process, this type of heat flux sensor can be produce easily. Furthermore, the sensitivity of their temperature sensors can be adjusted by varying the supply voltage of the Wheatstone bridges and thus the current flowing through each thermoresistance.

9. References

- [1] F Van der Graff, F. 1990, Heat flux sensors, in Ricol, T. and Scholz, J. (eds), Thermal Sensors 4, VCH, Weinheim, Germany-(1990) 297–322.
- [2] J M Devisme, T Langlet, O Douzane, J M Roucoult, M Quéneudec, *Int. J. Therm. Sci.* **40** (2001) 205-215
- [3] A V Mityakov, S Z Sapozhnikov, V Y Mityakov, A A Snarskii, M I Zhenirovsky, J J Pyrhonen, *Sens Actuators A*, **176** (2012) 1-9.
- [4] M Khaled, B Garnier, F Harambat, H Peerhossaini, *Meas. Sci. Technol.*, **21** (2010) 025903
- [5] J P Bardon, Y Jarny, « Procédé et dispositif de mesure en régime transitoire de température et flux surfacique » Patent n° 94.01996, Feb 22th 1994
- [6] J V Beck, B Blackwell, C R St Clair, Jr, *Inverse Heat Conduction*. Wiley, Inc. New York, 1985
- [7] A Saidi, J Kim, *Exp Therm. Fluid Sci.*, **28** (2004) 903-908
- [8] J V Beck, B Blackwell, A H Sheikh, *Int. J. Heat Mass Transfer*, **39** (1996) 3649-3657
- [9] B Blackwell, J V Beck, *Int. J. Heat Mass Transfer*, **53** (2010) 753-759
- [10] G Blanc, M Raynaud, T H Chau, *Rev Gén Therm.*, **37** (1998) 17-30
- [11] B Bourouga, V Goizet, J P Bardon, *Int. J. Therm. Sci.*, **39** (2000) 96-109
- [12] J P Prenel, F Lanzetta, E Gavignet, Y Bailly, B Serio, P Nika, L Thiery, *Encyclopedia of Sensors* volume X: Pages (1-29)
- [13] L Thiery, Y Bailly, F Lanzetta, H Gualous, E Gavignet, *Rev Gén Therm.*, **37** (1998) 60-73
- [14] D Hamadi, B Garnier, H Willaime, F Monti, H Peerhossaini, *Lab on a chip*, **12** (2012) 652-658
- [15] A G Kozlov, *Int. J. Therm. Sci.*, **45** (2006) 41-50
- [26] M A Shannon, T M Leicht, P Hrnjak, N Miller, F Khan, *Sens. Actuators A*, **88** (2001) 164-177
- [17] N R Keltner, B L Bainbridge, J V Beck, *J. Heat Transfer*, **110** (1988) 42
- [18] J E Doorly, *J. Turbomach.*, **110** (1988) 242
- [19] E Piccini, S M Guo, T V Jones, *Meas. Sci. Technol.*, **11** (2000) 342-349.
- [20] H D Bhatt, R Vendula, S B Desu, G C Fralick, *thin solid films*, **342** (1999) 214-220
- [21] S K Mukherjee, M K Sinha, B Pathak, S K Rout, L Ng, *Thin Solid Films*, **518** (2010) 5839-5854
- [22] J J Atherton, M C Rosamond, S Johnstone, D A Zeze, *Sens. Actuators* doi: 10.1016 / i.sns. 2011.01.001
- [23] J Ewing, A Gifford, D Hubble, P Vlachos, A Wicks, *Meas. Sci. Technol.*, **21** (2010) 10520
- [24] D G. Holmberg, T E Diller, *J. Fluids Eng.*, **117** (1995) 659
- [25] S H Oh, K C Lee, J Chun, M Kim, J Micromech, *J. Micromech. Microeng.*, **11** (2001) 221-225
- [26] L W Langley, A Barnes, G Matijasevic, P Gandhi, *Micro-elect Journal*, **30** (1999) 1163-1168
- [27] G Ravalitera, M Cornet, B Duthoit, P Thery, *Revue Phys. ital.*, **17** (1982) 177-185
- [28] T Moussa, B Garnier, H Peerhossaini, Proceedings of the ASME 2012 11th Biennial Conference on Engineering Systems Design and Analysis, Nantes France, July 2-4 2012

Acknowledgments

This research program has been supported by the Interdisciplinary Program of Energy from CNRS (PIEnergie CNRS/ PE Capinov) and the Vendee General Council